The Polarised Charge–Exchange Reaction $\vec{d} + p \to (pp)_{^1S_0} + n$

A. Kacharava, E. Steffens, S. Yaschenko
Physikalisches Institut II, Universität Erlangen–Nürnberg, 91058 Erlangen, Germany

V.V. Glagolev
Joint Institute for Nuclear Research, Laboratory of High Energy, 141980 Dubna, Russia

R. Engels, R. Gebel, M. Hartmann, V. Hejny, I. Keshelashvili, I. Lehmann, B. Lorentz, Y. Maeda, A. Mussgiller, H. Ohm, D. Prasuhn, F. Rathmann, R. Schleichert, H. Seyfarth, H.J. Stein, H. Ströher, A. Wrońska
Institut für Kernphysik, Forschungszentrum Jülich, 52425 Jülich, Germany

S. Dymov, V. Komarov, A. Kulikov, V. Kurbatov, G. Macharashvili, S. Merzliakov, Yu. Uzikov*, B. Zalikhanov
Joint Institute for Nuclear Research, LNP, 141980 Dubna, Russia
**delegated from Kazakh National University, 480078 Almaty, Kazakhstan*

N. Amaglobeli, B. Chiladze, M. Nioradze
High Energy Physics Institute, Tbilisi State University, 380086 Tbilisi, Georgia

A. Khoukaz, N. Lang
Institut für Kernphysik, Universität Münster, 48149 Münster, Germany

H. Paetz gen. Schieck
Institut für Kernphysik, Universität zu Köln, 50937 Köln, Germany

S. Barsov, M. Mikirtytchiants, V. Nelyubin, A. Vassiliev
High Energy Physics Department, Petersburg Nuclear Physics Institute, 188350 Gatchina, Russia

C. Wilkin
Physics and Astronomy Department, University College London, London WC1E 6BT, United Kindom

for the ANKE Collaboration

Jülich, March 27, 2003

Abstract

During our study of the $pd \to n(pp)$ reaction in the backward direction at ANKE, we have acquired considerable expertise in measuring two protons at low relative momentum such that they are in the peak of the $^1S_0$ final state interaction . We now wish to exploit this technique, together with the possibilities offered by the acceleration of polarised deuterons at COSY, to measure the $\vec{d}p \to (pp)_{^1S_0}n$ charge–exchange reaction near the forward direction, *i.e.* where the four–momentum transfer t between the proton and neutron is small. The cross section and analysing power data can then be interpreted in terms of the amplitudes of the $np \to pn$ charge–exchange reaction and our results should provide information on the spin–spin terms in the amplitude in the energy range above 800 MeV (LAMPF) and up to the maximum beam energy per nucleon achievable at COSY, *viz.* 1150 MeV. A possible extension using a vector polarised beam on a polarised target is also envisaged.

Contents

1 Introduction

The complete description of the NN interaction requires precise data as input to phase–shift analyses (PSA), from which the scattering amplitudes can be reconstructed. The PSA generally requires experiments with both beam and target particles polarised in the initial state, as well as polarisation determination of final state particles [1]. Experiments of this type have been carried out for the pp system to about 3.0 GeV [2, 3]. Due to the absence of polarised neutron beams, there has been much less work done on spin observables in elastic np scattering above 800 MeV [4, 5]. As a consequence, the PSA for isospin $I = 0$ are poorly tested in this region. Precise new data are needed in order to try to bridge the gap with the pp system. Information can be obtained on the spin–dependent np elastic amplitudes near the backward direction (the charge–exchange region) by measuring the charge–exchange breakup of polarised deuterons on an unpolarised hydrogen target.

1.1 Scientific motivation

We propose to study the spin structure of the amplitudes of the elementary $np \to pn$ charge–exchange (CE) process *via* the deuteron–induced $\vec{d}p \to (pp)n$ reaction, where the proton in the deuteron acts largely as a spectator. The aim is to enhance substantially the existing np data base above $T_n = 800$ MeV at small angles θ between incoming neutron and outgoing proton. While the ongoing proton–induced deuteron breakup experiment [6] aims at an investigation of short–range features of the deuteron structure by looking at high–momentum transfer, the new proposal focuses on the region of small four–momentum transfer t between the proton and neutron, where the cross sections are much larger.

The possibility of using the CE reaction on the unpolarised deuteron in order to determine of the spin–dependent part of the elementary CE process was emphasised already in 1951 by Pomeranchuk [7]. The effect can be understood qualitatively as follows. The two nucleons in the deuteron are in $I = 0$, $^3\mathrm{S}_1$ or $^3\mathrm{D}_1$. The spatial and spin states are symmetric so that, by the generalised Pauli principle, the isospin state is antisymmetric. In the charge–exchange reaction at 0°, the transition to a spin antisymmetric $^1\mathrm{S}_0$ state of two protons therefore requires a spin flip. The overall intensity of the spin–dependent parts of the elementary $np \to pn$ CE amplitude can thus be inferred from the probability of the dp CE process. Furthermore, it has been shown that by measuring the deuteron tensor analysing powers it is possible to separate the intensities of the different spin amplitudes [8, 9]. Under special kinematic conditions (scattering angle θ close to zero and momentum transfer $t \sim 0$), the dp CE differential cross section is actually fully determined by the spin–dependent parts of the elementary $np \to pn$ amplitude.

The experimental programme is divided into two parts:

1. The first stage will utilise unpolarised and tensor polarised deuteron beams incident on an unpolarised hydrogen cluster target. The differential cross section gives only the overall intensity of the spin–dependent parts of the elementary CE process. Tensor polarised deuteron beam enables us to separate the absolute values of three spin–dependent amplitudes.

2. Using transversely polarised deuterons incident on a polarised internal hydrogen gas target and measuring the spin–correlation coefficient opens the possibility of obtaining the relative phase between amplitudes.

The present proposal covers only the first part. It is important to note that both polarised and unpolarised deuteron beams will be utilised concurrently. The study will eventually

also include measurements of spin–correlation parameters, once the polarised internal target for ANKE has been commissioned.

1.2 Determination of the scattering matrix

1.2.1 Scattering amplitudes

The amplitude of the elementary $np \to pn$ reaction in the cm system can be written in terms of five scalar amplitudes

$$f_{np} = \alpha + i\gamma(\boldsymbol{\sigma}_n + \boldsymbol{\sigma}_p)\mathbf{n} + \beta(\boldsymbol{\sigma}_n \cdot \mathbf{n})(\boldsymbol{\sigma}_p \cdot \mathbf{n}) + \delta(\boldsymbol{\sigma}_n \cdot \mathbf{m})(\boldsymbol{\sigma}_p \cdot \mathbf{m}) + \varepsilon(\boldsymbol{\sigma}_n \cdot \mathbf{l})(\boldsymbol{\sigma}_p \cdot \mathbf{l}), \quad (1)$$

where $\boldsymbol{\sigma}_n$ and $\boldsymbol{\sigma}_p$ are the Pauli matrices for neutron and proton, respectively. The orthogonal unit vectors are defined in terms of the initial ($\mathbf{k}$) and final ($\mathbf{k}'$) momenta as

$$\mathbf{n} = \frac{\mathbf{k} \times \mathbf{k}'}{|\mathbf{k} \times \mathbf{k}'|}, \quad \mathbf{m} = \frac{\mathbf{k}' - \mathbf{k}}{|\mathbf{k}' - \mathbf{k}|}, \quad \mathbf{l} = \frac{\mathbf{k}' + \mathbf{k}}{|\mathbf{k}' + \mathbf{k}|}.$$

The amplitudes are normalised such that the elementary $np \to pn$ differential cross section has the form

$$\left(\frac{d\sigma}{dt}\right)_{np\to pn} = I_{np} = |\alpha|^2 + |\beta|^2 + 2|\gamma|^2 + |\delta|^2 + |\varepsilon|^2, \quad (2)$$

where α is the spin–independent amplitude, γ is related to the spin–orbit coupling, and β, δ, and ε are the spin–spin amplitudes. The one–pion–exchange pole is contained purely in the δ amplitude and this gives rise to its very rapid variation with momentum transfer.

For low excitation energy $E_{pp} < 3$ MeV of the final pp pair, and at low transferred three-momentum ($q \approx 0$) from proton to neutron (or from deuteron to diproton), the charge exchange reaction $dp \to (pp)n$ mainly excites the $^1S_0$ state of the final pp system. In impulse approximation, *i.e.* single $np \to pn$ scattering, the resulting amplitude depends only upon the spin–dependent parts of f_{np}, *i.e.* β, γ, δ and ε [9]. The form factor describing the transition from a deuteron with spin–projection λ to a ($^1S_0$)–state of the final pp pair contains two terms

$$S^+(k, \tfrac{1}{2}q) = F_S(k, \tfrac{1}{2}q) + \sqrt{2}F_D(k, \tfrac{1}{2}q), \quad (3)$$

$$S^-(k, \tfrac{1}{2}q) = F_S(k, \tfrac{1}{2}q) - \frac{1}{\sqrt{2}}F_D(k, \tfrac{1}{2}q). \quad (4)$$

The S^+ and S^- denote the longitudinal ($\lambda = 0$) and transverse ($\lambda = \pm 1$) form factors. The matrix elements F_S and F_D can be expressed by the S and D components of the deuteron wave function $u(r)$ and $w(r)$ and the $pp(^1S_0)$–scattering wave function $\psi_k^{(-)}(r)$ as

$$F_S(k, \tfrac{1}{2}q) = \langle \psi_k^{(-)} | j_0(\tfrac{1}{2}qr) | u \rangle, \quad (5)$$

$$F_D(k, \tfrac{1}{2}q) = \langle \psi_k^{(-)} | j_2(\tfrac{1}{2}qr) | w \rangle. \quad (6)$$

Here k is the pp relative momentum, corresponding to an excitation energy $E_{pp} = k^2/m$, where m is the proton mass. Denoting the ratio of the transition form factors by

$$R = \frac{S^+(k, \tfrac{1}{2}q)}{S^-(k, \tfrac{1}{2}q)} \quad (7)$$

and

$$I = |\beta|^2 + |\gamma|^2 + |\varepsilon|^2 + |\delta|^2 R^2, \quad (8)$$

for the sum of squared amplitudes, differential cross section, tensor analysing powers, and spin–spin correlation parameters $C_{y,y}$, $C_{x,x}$, $C_{z,z}$ of the $dp \to (pp)_{^1S_0}n$ reaction assume the forms [11, 12]

$$\frac{d^4\sigma}{dtd^3k} = \frac{1}{3} I \left\{ S^-(k, \tfrac{1}{2}q) \right\}^2 , \tag{9}$$

$$I\, T_{20} = \frac{1}{\sqrt{2}} \{ |\gamma|^2 + |\beta|^2 + |\delta|^2 R^2 - 2|\varepsilon|^2 \} , \tag{10}$$

$$I\, T_{22} = \frac{\sqrt{3}}{2} \{ |\gamma|^2 + |\beta|^2 - |\delta|^2 R^2 \} , \tag{11}$$

$$I\, C_{y,y} = -2\Re(\varepsilon^* \delta) R, \tag{12}$$

$$I\, C_{x,x} = -2\Re(\beta^* \varepsilon), \tag{13}$$

$$I\, C_{z,z} = -2\Re(\delta^* \beta) R . \tag{14}$$

Thus, a measurement of the differential cross section, T_{20}, and T_{22} will allow us to extract the $|\beta|^2 + |\gamma|^2$, $|\delta|^2$, and $|\varepsilon|^2$ intensities over a range in q near the forward direction. Since γ vanishes at $q = 0$ and is generally small in our energy and angular domain, this means that our experiment essentially leads to a determination of the absolute values of the spin–spin amplitudes in np charge exchange. It is important to note that amplitude analysis at 800 MeV shows that the spin–independent term α is much smaller than β [13].

In order to get the relative phases of the spin–spin amplitudes requires spin–correlation and spin–transfer information and for this the situation simplifies enormously in the forward direction.

1.2.2 Collinear kinematics

In collinear kinematics, where all momenta lie along the beam direction, $\mathbf{k} = \mathbf{k}'$, the number of scalar amplitudes in Eq. (1) reduces from five to three because of the azimuthal symmetry. In this limit

$$\delta = \beta \qquad \text{and} \qquad \gamma = 0 . \tag{15}$$

At $q = 0$ the D–wave form factor vanishes, $R = 1$, and also $T_{22} = 0$. One then finds from Eqs. (9-13)

$$\frac{d^4\sigma}{dtd^3k} = \frac{1}{3} \{ |\varepsilon|^2 + 2|\beta|^2 \} F_S^2(k, 0), \tag{16}$$

$$I = 2|\beta|^2 + |\varepsilon|^2, \tag{17}$$

$$I\, T_{20} = \sqrt{2} \{ |\beta|^2 - |\varepsilon|^2 \}, \tag{18}$$

$$I\, C_{y,y} = I\, C_{x,x} = -2\Re(\varepsilon \beta^*). \tag{19}$$

Furthermore

$$I\, C_{xz,y} = -I\, C_{yz,x} = 3\Im(\beta \varepsilon^*). \tag{20}$$

Having found the moduli of the amplitudes β and ε, a measurement of the spin–spin correlation factor $C_{y,y}$ yields the cosine of the relative phase, $\cos(\varphi_\varepsilon - \varphi_\beta)$. This will require a vector polarised deuteron beam and a hydrogen target. In order to resolve the remaining ambiguity, one has for example to measure also the sign of the spin–tensor coefficient $C_{xz,y}$. The deuteron charge exchange experiment is, of course, completely insensitive to the value of α.

1.2.3 Closure approximation

Integrating Eq. (16) over the full phase space in d^3k, one can obtain closure sum rules that are insensitive to the details of the final pp interaction [14]. For example, at $q = 0$ one finds that

$$\left(\frac{\mathrm{d}\sigma}{\mathrm{d}t}\right)_{dp\to(pp)n} = \frac{1}{3}\left(2|\beta|^2 + |\varepsilon|^2\right)\,[2 + P_D]\ , \tag{21}$$

$$T_{20}\left(\frac{\mathrm{d}\sigma}{\mathrm{d}t}\right)_{dp\to(pp)n} = \frac{2\sqrt{2}}{3}\left(|\beta|^2 - |\varepsilon|^2\right)\,\left[1 - \tfrac{9}{10}P_D\right]\ , \tag{22}$$

where P_D is the D–state probability in the deuteron. Although the region where $t \approx 0$ would represent only a small part of our total data sample, it is interesting to note that the closure approximation describes to within about 10% the non–charge exchange inelastic scattering cross section $pd \to p(pn)$ [15] at GeV energies within the Glauber–Franco theory [16].

1.3 Elastic np scattering

Below we give a brief overview of the existing data on np data and their interpretation. The summary is divided into three sections, covering

- np elastic and quasi–elastic data (Sec. 1.3.1),
- np elastic charge–exchange (CE) data (Sec. 1.3.2), and
- data on deuteron–induced charge–exchange (CE) reaction $dp \to (pp)n$ (Sec. 1.3.3).

1.3.1 Elastic and quasi–elastic np scattering

During the 1980's a world–wide experimental effort was undertaken to obtain np elastic scattering data at all accelerators where a polarised neutron beam was available.

Elastic np scattering below 1.1 GeV:
Low energy np spin observables were measured at TRIUMF (200 – 500 MeV) [17], at PSI (200 – 560 MeV) [18], and at LAMPF (480 – 800 MeV) [19]. Data at higher energies were mainly obtained at SATURNE–2 (800 – 1100 MeV) [20]. When measurements of the np transverse and longitudinal total cross section differences, $\Delta\sigma_T = \sigma(\uparrow,\uparrow) - \sigma(\uparrow,\downarrow)$ and $\Delta\sigma_L = \sigma(\stackrel{\rightarrow}{\rightarrow}) - \sigma(\stackrel{\rightarrow}{\leftarrow})$, cited in Table 1, are combined with those for pp collisions, one can deduce the imaginary parts of the amplitudes β and ε in the forward direction. The conditions for the twelve np spin–dependent observables at SATURNE–2 in the cm scattering angle range 21° to 150° are summarised in Table 1, the corresponding references are given in ref. [21].

The normalised differential cross section $d\sigma/dt$ for elastic np scattering was measured in a smaller angle range, $4° < \theta_{\rm lab} < 10°$, at 14 different energies between 378 and 1135 MeV by the IKAR collaboration at Saturne [29]. They also measured the analysing power A_{00n0} at a few angles at five energies. These data allowed them to extract the ratio of the real to imaginary part of the forward spin–independent scattering amplitudes.

Elastic np above 1.1 GeV: The np data at higher energies obtained are listed in Table 2. They were measured with unpolarised neutron beams with large energy spread, and with polarised (unpolarised) protons scattered off unpolarised (polarised) deuterium targets. In addition to these data, two A_{00nn} points were measured at the ANL–ZGS [30]

Observable	T (GeV)	range θ_{cm} (deg)	# points
$\Delta\sigma_T$	0.630 – 1.100	—	11
$\Delta\sigma_L$	0.312 – 1.100	—	10
A_{00n0}, A_{000n}	0.312 – 1.100	21 – 150	766
A_{00nn}	0.744 – 1.100	25 – 150	335
A_{00kk}	0.312 – 1.100	29 – 148	256
A_{00sk}	0.744 – 1.100	26 – 148	219
D_{0n0n} and K_{0nn0}	0.800 – 1.100	48 – 86	30
$D_{0s''0k}$	0.800 – 1.100	42 – 77	20
$K_{0s''k0}$ and N_{0nkk}	0.800 – 1.100	42 – 77	20
$K_{0s''s0}$ and N_{0nsk}	0.800 – 1.100	42 – 77	20

Table 1: Summary of *np* observables measured at SATURNE–2 in the notation of Ref. [21].

using the 6 GeV/c polarised neutron beam. Spin–dependent total cross section differences $\Delta\sigma_L$ were determined from ANL–ZGS *pd* and *pp* measurements [31]. Another measurement used a quasi–monochromatic polarised neutron beam and a polarised proton target at the JINR Synchrophasotron [32].

Laboratory	Observable	Beam	T (MeV)	Reference
LBL BEVATRON	A_{000n}	n	1731 ± 468	[22]
			2684 ± 483	
ANL–ZGS	A_{000n}	n	2205 ± 954	[23]
ANL–ZGS	A_{00n0}	$\vec{p}$	1030	[24]
			1271	[25]
			2205	[26]
KEK	A_{000n}	p	1109	[27]

Table 2: *np* observables measured at various laboratories.

Quasi–elastic *np***:** The maximum neutron beam energy obtained from stripping accelerated deuterons at SATURNE–2 was close to 1.1 GeV. Data at higher energies were obtained using quasi–elastic scattering of polarised protons on a solid polarised deuteron target, made of ^{6}LiD [28]. The spin–dependent observables were measured with proton beams in the energy range of 1.1–2.4 GeV [5]. These measurements are summarised in Table 3. The quasi–elastic *pn* results for protons scattered on weakly bound neutrons in deuterons and in ^{6}Li nuclei show good agreement with *np* elastic scattering data. They improve significantly the existing spin–dependent database and constrain the PSA from $\theta_{cm} = 54$ to 130° angular region. Nevertheless, the $I = 0$ PSA above 1.1 GeV are not well tested.

It should be noted that the existing *np* data around and above 1.1 GeV are scarce. Despite the large nucleon–nucleon programs carried out at intermediate–energy laboratories, these data do not cover small scattering angles ($\theta_{lab} < 4°$). The PSA are therefore poorly tested at small forward angles and additional data are highly desirable to provide further insight [2].

Observable	Target	T (GeV)	range θ_{cm} (deg)	Points
A_{00n0}	^{6}LiD	1.1–2.4	54–130	58
	^{6}LiH	1.1	54–130	22
		2.1	71–117	9
A_{00nn}	^{6}LiD	1.1	83–127	7
		1.6	82–112	3
D_{n0n0}	^{6}LiD	1.1–2.4	88–127	15
	^{6}LiH	1.1–2.4	90–127	14

Table 3: Listing of SATURNE–2 data obtained from polarised protons scattered quasi–elastically off ^{6}LiD and ^{6}LiH targets. (Data from ref. [5].)

1.3.2 np elastic charge–exchange (CE) data

Numerous experimentalists were attracted to $np \to pn$ charge–exchange measurements in the sixties by the idea of extrapolating to the pion pole. For example, Palevsky et al. [33] measured np CE scattering at incident neutron momenta of 2.83 GeV/c and 3.67 GeV/c. It was found that the distributions in transverse momentum ($p_\perp = p_0 \cdot sin\theta \simeq \sqrt{-t}$) were sharply peaked at zero momentum transfer. More systematic studies were carried out in an experiment at the Princeton–Pennsylvania Accelerator (PPA), using a neutron beam with momenta between 600 and 2000 MeV/c [34]. The differential cross sections show a sharp change in the slope of $d\sigma/dt$ and reveal a very narrow forward peak which is much sharper than that in pp elastic scattering. Since the slope of the cross section at small t values is of the order of m_π^{-2} (m_π is pion mass), it is natural to associate it with the one pion–exchange (OPE) mechanism, though distortion is important to avoid the amplitude vanishing at $t = 0$. The pion exchange peak is, in fact, seen over a wide variety of neutron momenta up to at least 65 GeV/c [35, 36, 37, 38, 39, 40]. A fit to the differential cross section $d\sigma/dt$ at $t = 0$ yields a $1/p^2$ behaviour, where p is the laboratory momentum of the incoming neutron [33]. Later experiments confirmed the normalisation at 1.73 GeV/c [37].

In the case of the polarised data, the analysing power and a few spin–transfer observables have been measured in the np CE region at several energies from 485 MeV up to 790 MeV using the LAMPF polarised neutron beam [41, 42].

1.3.3 Deuteron–induced charge–exchange (CE) reaction dp $\to$ (pp)n

The deuteron–induced CE breakup reaction $dp \to (pp)n$ was studied in the 1 m hydrogen bubble chamber (HBC) at the 3.34 GeV/c deuteron beam of the JINR Synchrophasotron. The first results, on a relatively small fraction of the processed events, were published [43, 44]. The authors returned to this problem, exploiting the final charge–exchange statistics of over 10^5 events [45]. Their aim was to estimate the possibilities and limitations of a counter experiment STRELA [46], which had been proposed to study the spin–dependent part of the np charge–exchange amplitudes using the JINR Nuclotron deuteron beam in the momentum range from 3.0 to 4.0 GeV/c. However, the information extracted from the bubble chamber experiment at small angles ($\leq 3^\circ$) is not sufficient to observe the behaviour of the differential cross section close to 0°.

The deuteron tensor analysing powers in the $dp \to (pp)n$ reaction should be especially strong in regions where the pp excitation energy is small and the momentum transfer to the neutron is of the order of pion mass or less [8, 9]. This reaction provides information equivalent to that of $(\vec{n}, \vec{p})$ [47], without the need to measure the polarisation of the outgoing particles. It has also been used as the basis of an efficient analyser of deuteron–

tensor polarisations at intermediate energies [11]. The impulse approximation predictions have been tested at energies of $T_d = 200$ MeV and 350 MeV [48] with the EMRIC apparatus and at $T_d = 1.6$ and 2.0 GeV with the SPES4 magnetic spectrometer [49, 50] [1]. The kinematics of the latter experiments are quite close to those of the present proposal, though it should be noted that the acceptance of the SPES4 spectrometer for two protons was not sufficiently well understood to allow for the extraction of absolute cross sections. Nucleon–nucleon charge exchange amplitudes were therefore introduced into the analysis and, after testing on the nucleon, were used in the study of spin–isospin excitations in nuclei. The main purpose of these experiments, in fact, was the investigation of the spin structure of the Δ excitation on a nucleon and in a nucleus.

The main effort of the other deuteron breakup experiments at large momentum transfers was focused on the study of the reaction mechanisms and deuteron structure at small distances (for a review see Ref. [51]).

Since we can measure normalised cross sections, our experiment will be the first that can provide data necessary to determine the spin–dependent part of the elementary $np \to pn$ CE process in the energy range of about 1 GeV by investigation of the deuteron–induced CE reaction.

1.4 Why the suggested experiment is unique

There are a large number of positive features in the proposed experiment:

1. The large acceptance of the FD system at ANKE for the $dp \to (pp)n$ charge–exchange reaction provides advantageous experimental conditions. The transition to collinear kinematics can be approached in a symmetric way near zero degree (see Fig. 2).

2. In contrast to SPES4, the spectrometer acceptance for two particles is understood quantitatively.

3. As shown in more detail in Sec. 3.2, our set–up provides:

   - High count rates,
   - good beam and target overlap, thus giving a small interaction volume,
   - the *internal* target experiment provides for good background conditions,
   - as shown in Fig. 2, our set–up is sensitive to a number of different reactions.

4. The polarised deuteron beam at COSY has been successfully accelerated (Sec. 2.3). The different polarisation states, required for the experiment proposed here, have already been delivered for previous experiments.

5. Generally, *pn* data obtained with a pure gas target, either an unpolarised cluster target, or at a later stage an isotopically pure polarised gas target (see Sec. 6.1), are considered superior compared to those from a ^{6}LiD target, used at Saturne [28].

2 Experimental set–up

2.1 Detection System

We consider here the possibility of studying the deuteron–induced CE breakup reaction using the ANKE spectrometer [52]. Two fast protons, emitted in a narrow forward cone

[1] Double scattering effects are generally small at low angles and can be estimated in an eikonal approach [9].

with momenta around half that of the deuteron beam, will be detected by the Forward Detector (FD) system of the ANKE set–up. The detection of proton pairs in the forward direction was already achieved in our proton–induced deuteron breakup experiment, though it should be stressed that this was in the regime of large momentum transfer [6].

In Fig. 1 those parts of the spectrometer are shown that are relevant for the present experiment. The deuterons stored in the COSY ring will impinge on a hydrogen cluster–jet target. The hodoscope, containing two layers of 8 and 9 vertically oriented scintillators, will provide a trigger signal and energy loss measurement. It allows us also to determine differences in the arrival times for particle pairs hitting different counters. The system of Čerenkov counters facilitates discrimination of the forward–emitted protons from the deuterons. Three multi–wire chambers are utilised to reconstruct the particle tracks, from which subsequently the momenta are determined. The silicon telescope system will be employed to measure the vector polarization of the deuteron beam (Sec. 4.2.1).

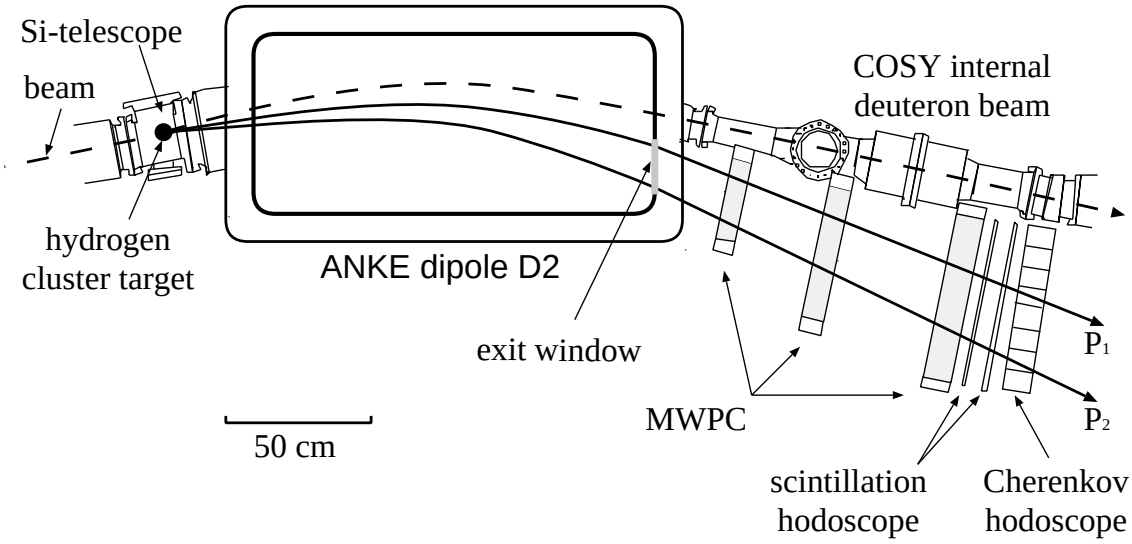

Figure 1: Top view of the experimental set–up showing the forward detection system of the ANKE spectrometer.

2.2 Acceptance of the forward system

The horizontal acceptance of the set–up for $T_d = 1.2$ GeV and 2.23 GeV (maximum at COSY) is shown in Fig. 2. The vertical acceptance corresponds to $\pm 3.5^\circ$. Deuterons from dp elastic scattering within the ANKE acceptance are also indicated. These events will be used for luminosity determination and detector calibrations. Also shown are pions and tritons from the $dp \to t\pi^+$ reaction, and ^{3}He from the isospin–related $dp \to {}^3\mathrm{He}\,\pi^0$ reaction. Since the tensor analysing power T_{20} has been measured for forward and backward production as a function of energy [53], these reactions can be used as a polarimeter for the deuteron beam.

A measurement of T_{22} requires to detect scattering angles away from zero degree, where this observable vanishes. Making use of the transverse positioning capability of the D2 magnet, the angle interval accepted in the forward detector can be optimised.

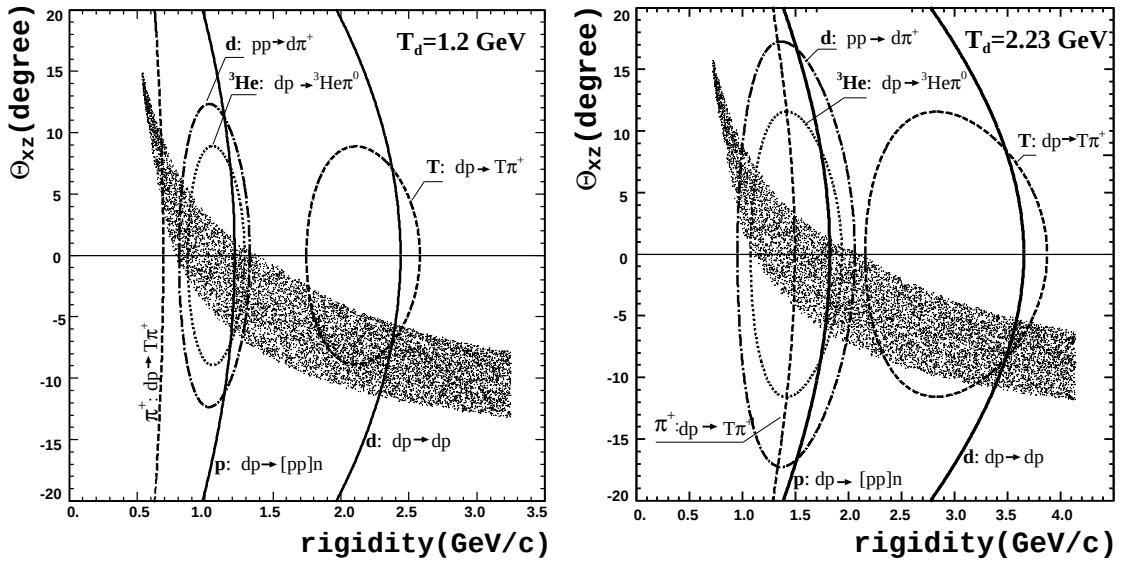

Figure 2: MC simulation of the acceptance of the ANKE set–up, showing angle versus rigidity (momentum/charge). θ_{xz} denotes the scattering angle of the emitted particle projected onto the median plane of the spectrometer. The curves show kinematic loci for π^+, p, d, t, and ^{3}He, from the indicated processes. The brackets, *e.g.* $[pp]$, denote a forward proton pair with zero excitation energy.

2.3 The COSY deuteron beam

Measurements with unpolarised and polarised deuterons impinging on an unpolarised hydrogen cluster target [54] will be performed in order to investigate the spin–averaged differential cross section. The target thickness is about $\sim 5 \times 10^{13}$ atoms/cm^2 and up to 5×10^{10} deuterons may be stored in the COSY ring [55]. The maximum deuteron energy is 2.23 GeV ($p_d = 3.65$ GeV/c).

The experiment will use the polarised deuteron beam from the COSY ion source. For that purpose the procedure employed in the SPIN@COSY experiment in February 2003 will be adopted. The scheme consists of five different polarisation states, one unpolarised state and four combinations of vector and tensor polarisation, as shown in Table 4. For each

	theoretical maximum			
	vector	tensor		
Mode	P_z	P_{zz}	Intensity $[I_0]$	Measured P_z
1	0	0	1	0.00
2	$-2/3$	0	1	-0.41
5	$-1/3$	-1	1	-0.35
10	$+1$	$+1$	2/3	$+0.57$
11	-1	$+1$	2/3	-0.70

Table 4: Modes of the polarised deuteron ion source. The intensity modulations between the different modes constitute a compromise in order to achieve higher polarisations. I_0 refers to the maximum number of deuterons delivered by the source and stored in COSY. At the deuteron energies of our experiment, $I_0 = 10^9$ deuterons are expected. The last column shows the vector polarisations measured during the SPIN@COSY experiment.

injection into COSY, the polarised ion source can be switched to a different polarisation state. The duration of a cycle is sufficiently long to ensure stable conditions for the injection of the next state. After the fifth state, the source will be reset to the first mode and the pattern is repeated. The ANKE data acquisition system receives status bits from the source, latched during injection, that ensure the correct identification of the polarisation states during the experiment.

The vector polarisation of the different states can be measured at the low energy polarimeter in the injection beamline between the JULIC pre–accelerator Cyclotron and the injection into COSY. The tensor polarisation will be measured using the ANKE spectrometer (see Sect. 4.2.2). Because of their small magnetic moment, deuterons encounter no depolarising resonances in the energy range of COSY and are unlikely to be depolarised. This was recently tested for a vector polarised beam, at least qualitatively, during the SPIN@COSY experiment. It should be noted, that the present experiment will be the first one that provides at the same time a measurement of vector and tensor polarisation of the deuteron beam stored in COSY.

Table 5 shows eleven deuteron polarisation states presently available from the source. The combinations of states which do not involve an exchange of rf transitions are: (1, 2, 4, 10, 11), and (1, 2, 5, 10, 11). Exchange of rf transitions requires the breaking of the

Mode	vector P_z	tensor P_{zz}	Intensity $[I_0]$
1	0	0	1
2	$-2/3$	0	1
3	$+2/3$	0	1
4	$+1/3$	$+1$	1
5	$-1/3$	-1	1
6	$+1/3$	-1	1
7	$-1/3$	$+1$	1
8	0	-2	2/3
9	0	$+1$	2/3
10	$+1$	$+1$	2/3
11	-1	$+1$	2/3

Table 5: Deuteron polarisation states available from the polarised ion source.

vacuum. Therefore, an interruption of polarised beam operation for at least one day, plus extra time for the subsequent retuning of the transitions, would be required for this to be done.

3 Measurements

As a first step, measurements with unpolarised deuterons [55] incident on the unpolarised cluster target [54] will be performed in order to compare the differential cross section with Eq. (9). The two fast protons, emitted into a narrow forward cone with momenta around half the deuteron beam momentum, will be detected in the ANKE forward detector system (Fig. 1). During the same data–taking period, in parallel to the unpolarised study, the polarised deuteron beam will allow us to carry out the first polarisation studies, where we intend to obtain a measurement of T_{20} and T_{22}, as given by Eqs. (10,11). For that aim, we will take data with the polarisation modes cycling, *e.g.* through states 1, 2, 5, 10, and 11, as indicated in Table 4.

Spin–correlation studies, such as the measurement of $C_{y,y}$, require a polarised proton target in addition to the polarised deuteron beam. These become possible after the commissioning of the polarised internal target. Even further in the future, measurements of $C_{z,z}$, which require longitudinally polarised beam and target are possible, once a Siberian snake and a special holding field magnet for the polarised target are in place (see Sec. 6).

3.1 Absolute normalisation

The absolute normalisation of the cross–section with an accuracy of about 5% requires accurate data from a known reaction within the detector acceptance. In previous experiments, our group has already used *pd* elastic scattering for this purpose, when analysing data from the first generation spectator detector at ANKE [56]. Due to the limited space in the old ANKE target chamber, only *pd* events from a fraction of the longitudinal extension ($\sim$ 12 mm) of the target could be detected in spectator counter. This resulted in a large uncertainty of the luminosity.

The second–generation spectator detector [56], mounted inside the new ANKE target chamber, circumvents this difficulty and recoil protons from *dp* elastic scattering over the full target length will be detected in coincidence with the forward deuterons. The telescope consists of three layers of double–sided structured silicon wafers of 65 μm, 300 μm, and 5 mm thickness, placed inside the vacuum chamber. Their high granularity, in combination with an individual read–out of each segment by dedicated chip–electronics, provides tracking information together with a high rate capability. Recoil protons from *dp* elastic scattering emitted from the target in the polar angle range of 45 to 90° can be detected. The larger detectors improve the recoil proton acceptance for a single telescope by about a factor of 10, compared to the previous set–up. Since all detectors are double–sided, the tracking capability over the energy range T_p = 2.5 to 30 MeV facilitates an installation close to an extended target. A complete telescope test measurement within the new target chamber will take place during the August 2003 beam–time.

The preliminary analysis of the *dp* data from the $dd \to \alpha\eta$ experiment in January 2003 [57], obtained using an unpolarised 2.345 GeV/c deuteron beam, revealed that the elastic deuteron peak is well separated from the protons originating from deuteron stripping, which possess about half the beam momentum in the single track momentum spectra (see left panel of Fig. 3). Taking into account the large cross section, we will use the high–quality elastic *dp* data from ref. [58] to obtain an absolute normalisation of $\sim$ 5% accuracy.

3.2 MC Simulation

3.2.1 FD acceptance for forward–emitted proton pairs

The MC simulations have been obtained using hydrogen bubble chamber (HBC) data [43] as a GEANT event generator. The simulations were carried out in order to estimate the efficiency of the ANKE forward detection system for registering two fast protons at small production angles. In addition, the probability of identifying the deuteron charge–exchange process among background reactions was obtained from the simulations.

The simulated two–proton CE events, accepted in the FD, are shown in Fig. 4. The upper panels show scattering angle *vs* excitation energy and momentum transfer, respectively. The lower panels illustrate how the cut on both angles $\theta_1 < 2°$ and $\theta_2 < 2°$ affects the number of events.

The HBC data were obtained using a 3.34 GeV/c deuteron beam, corresponding to a proton beam momentum of 1.67 GeV/c (T_p = 1.0 GeV) in the deuteron rest frame.

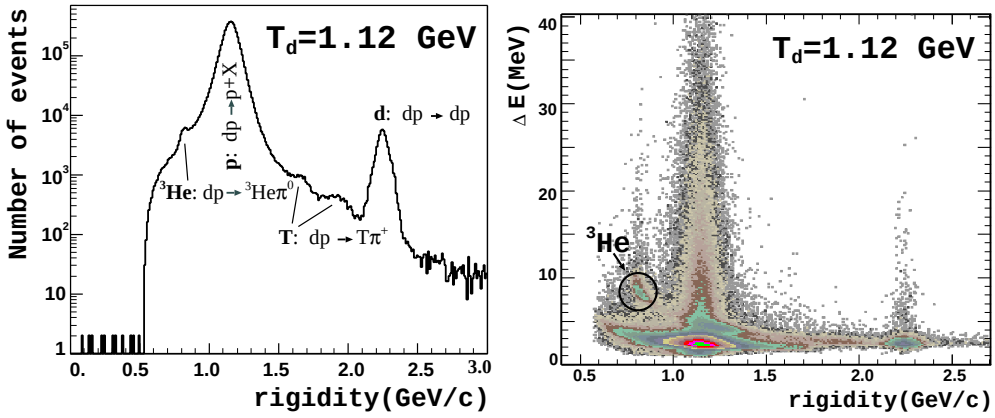

Figure 3: Left panel: Single track rigidity spectrum for the dp data obtained at ANKE using a deuteron beam of 2.345 GeV/c (T_d = 1.12 GeV) [57]. Right panel: Measured distribution of ΔE *vs* rigidity, indicating the clean identification of ^{3}He (encircled). Both spectra show preliminary data from the January 2003 beam time.

The main reaction at this energy is mesonless deuteron breakup. The events can be divided into two subgroups. The charge–exchange reaction was defined by the neutron momentum being higher than that of either of the two protons in the deuteron rest system. This definition provides a good separation of the charge exchange (CE) channel and direct charge–retention (DIR) channel events (see Ref. [43]). The corresponding cross sections are listed in Table 6.

Reaction type	Cross section [mb]
Total $dp \to$ X	82.89 ± 0.06
Total mesonless breakup $dp \to ppn$	37.2 ± 1.4
Mesonless charge–exchange $dp \to (pp)n$	6.4 ± 0.2

Table 6: Cross section data for the dp interaction at p_d = 3.34 GeV/c [43].

The total number of the real mesonless breakup events used in the GEANT event generator was 102778, of which 17524 events corresponded to CE reaction. The charged particles produced were considered as detected if, after passing the magnetic field of dipole D2, they were registered by a set of three multiwire proportional chambers and a scintillation–counter hodoscope. The simulation results for the charge–exchange reaction, as well as for the background processes, are listed in Table 7. The column labelled 'One–track events' corresponds to only one ejectile particle being detected in the FD, whereas for 'Two–track events', two ejectiles are detected simultaneously. The last column shows the number of two–track events, where both particles are emitted within 2° towards the direction of the incoming deuteron beam. Thus, the acceptance of the FD system for such proton pairs from the $dp \to (pp)n$ reaction results as $\varepsilon_{\rm acc} = 154/17524 = 8.8 \cdot 10^{-3}$.

3.2.2 Background and resolution

It is seen from Table 7 that the main physical background from single–track events is expected to originate from protons (see also Fig. 3). These can be eliminated through the detection of two charged particles in coincidence.

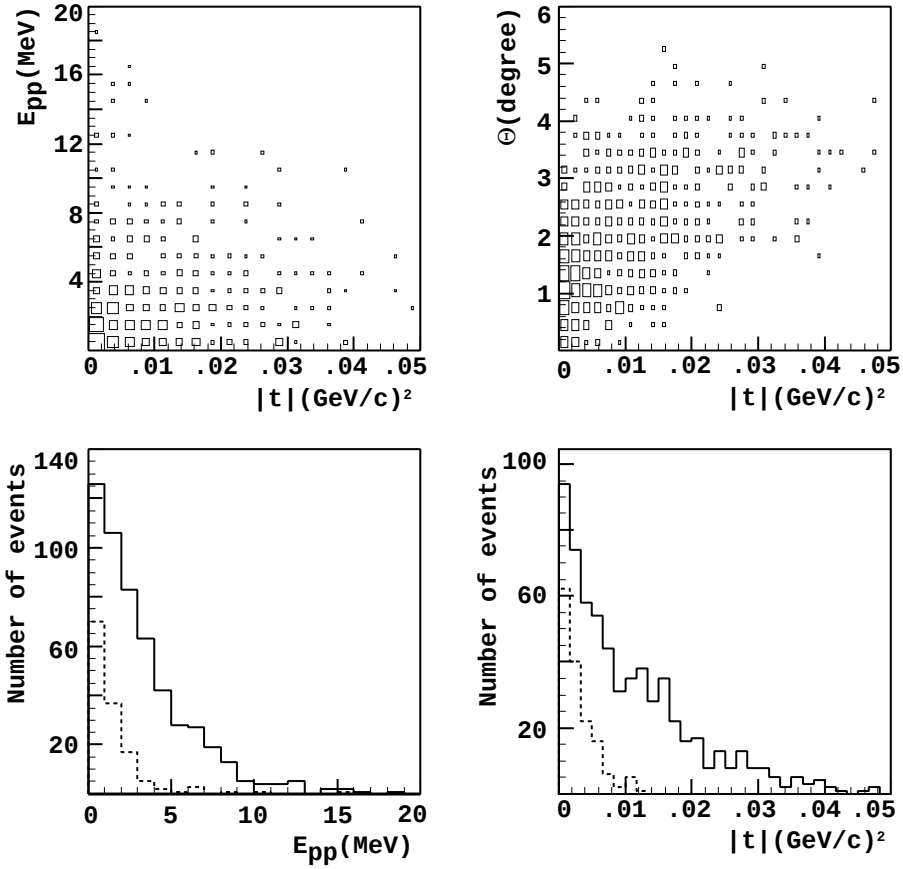

Figure 4: MC simulation based on HBC data at $p_d = 3.34$ GeV/c of the CE reaction accepted in the ANKE FD. The two upper panels show excitation energy E_{pp} and scattering angle vs momentum transfer $|t|$, respectively. The lower panels show histograms of E_{pp} and $|t|$ of the number of accepted events. The dashed histograms show events with the condition $\theta_1 < 2^\circ$ and $\theta_2 < 2^\circ$.

The main background among the two–proton events is expected to come from the $dp \to pp + n\pi$ reaction, but the missing–mass here is at least $m_n + m_\pi$. The quality of the separation can be judged from the recent analysis of the pd breakup process [6]. Figure 5 shows the missing–mass distribution of the selected proton pairs at T_p =0.8 GeV. The missing–mass spectrum reveals a well defined peak at the neutron mass, with an rms value of about 20 MeV/c^2, which is clearly separated from the pion production at 1.1 – 1.2 GeV/c^2.

The angular resolution for the track reconstruction with the new MWPC chambers is expected to be $\approx 0.3^\circ$ to 0.4°. The resolution already achieved in the excitation energy E_{pp} is better than 0.3 MeV for $E_{pp} < 3$ MeV [6]. The angular cut $\theta_1 < 2^\circ$ and $\theta_2 < 2^\circ$ is chosen such as not to lose events in this energy range. Collinear events with non–zero excitation energy are possible (Fig. 4). Even after imposing the E_{pp} cut, events with relative pp momentum close to the beam direction are more likely to dilute the analysing power signal [9], but this can be corrected for in the subsequent analysis.

One can conclude that the ANKE spectrometer is well suited for the study of the deuteron CE breakup reaction at small momentum transfer, thus facilitating a unique measurement of the spin–dependent part of the $np \to pn$ amplitude.

Reaction type	One–track events			Two–track events	$\theta_1 < 2^\circ$ and $\theta_2 < 2^\circ$
	p	d	π^+		
$dp \to (pp) + n$	6236	–	–	635	154
$dp \to (pn) + p$	13487	–	–	–	–
$dp \to pp + (n\pi^0)$	6822	–	–	278	35
$dp \to pp + (p\pi^-)$	768	–	–	124	12
$dp \to pp + (n\pi^+\pi^-)$	214	–	13	5	-
$dp \to p\pi^+ + (nn)$	5661	–	50	10	–
$dp \to dp$	–	1096	–	–	–
$dp \to dp + \pi^0(\pi^0)$	1024	598	–	69	12
$dp \to d\pi^+ + n(\pi^0)$	–	803	7	6	1
$dp \to \pi^+\pi^+ + nnn$	–	–	1	–	–

Table 7: Simulation results for the CE and background reaction in terms of the number of events detected in the FD system.

4 By–products of the investigation

4.1 Meson production reactions

In addition to measuring elastic dp scattering, we will also get data on the cross section and analysing powers of the $\vec{d}p \to dX$ reaction close to the forward direction. Inelastic events can be selected by a missing mass cut. Though, by isospin considerations $I_X = \frac{1}{2}$, it is likely that much of the cross section arises from the excitation of the Δ resonance in the deuteron. Deuteron analysing powers would allow further tests of theoretical models of $dp \to dN\pi$. Of interest are the two–track events where one measures both the deuteron and proton from the $dp \to dp\pi^0$ reaction. The theory of this process at low dp excitation energies is very close to that of $dp \to {}^3\mathrm{He}\,\pi^0$ [59].

4.2 Deuteron polarimeter reactions

4.2.1 Determination of the deuteron beam vector polarisation

The deuteron vector polarisation can be measured by analysing the azimuthal asymmetry of the forward scattered protons from quasi–free proton scattering on the proton target. For an unpolarised target, the $\vec{d}p \to (pn)p$ quasi–free analysing power is known from measurements of pp elastic scattering [60], and can be identified well using the ANKE spectator detector. A similar method was already used at JINR Dubna [62] and at Saturne [63]. For this purpose we can select single–track events, assuming that the spectator protons (with half the momentum of the deuteron beam) do not contribute to the asymmetry.

4.2.2 Polarimetry of the tensor polarised deuteron beam

The differential cross section and tensor analysing power T_{20} for $\vec{d}p \to {}^3\mathrm{He}\,\pi^0$ channel have been measured in the forward and backward directions at 19 energies between 0.5 and 2.2 GeV at Saturne [53]. Furthermore, full angular distributions of the cross section and all deuteron analysing powers have been measured from close to threshold at $T_d = 397$ MeV up to 430 MeV [64]. By charge independence, the analysing powers in this reaction should be identical to those in $\vec{d}p \to t\pi^+$, for which the cross section should be twice as large. The equality of the analysing powers has been tested at SPES4 for four angles using 1.1 and 1.3 GeV polarised deuterons [65].

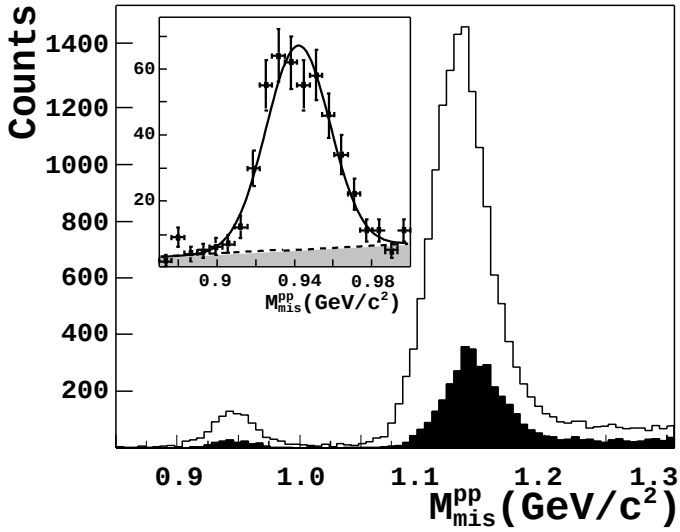

Figure 5: Missing–mass distribution [6] of all identified proton pairs (open histogram). The black histogram denotes identified pp pairs with excitation energy of less than 3 MeV. The inset shows the distribution near the neutron mass without particle identification for pairs with $E_{pp} < 3$ MeV. The background contribution is shown in grey. (Figure from ref [6].)

These pion–production reactions have large enough cross sections to detect them with good statistical accuracy. In Fig. 3 (arrows left panel), some enhancements in the spectrum are visible, which can be associated to $dp \to t\pi^+$ and $dp \to {}^3\mathrm{He}\,\pi^0$ events. The low momentum branch of the ^{3}He events is identified well from energy loss measurements (Fig. 3, right panel). Using these processes, a calibration of the deuteron tensor polarisation at COSY will become possible for the first time.

Detailed calculations of the figure of merit of the different polarimeter reactions are underway.

5 Requested Beam Time

5.1 Rate estimate

In order to estimate the expected count rate of fast two–proton pairs from the CE reaction and the required beam time for the measurements, we assume a luminosity of $L = 8 \cdot 10^{28}$ s^{-1}cm^{-2} ($\approx 1 \cdot 10^9$ stored deuterons, $f_{\mathrm{rev}} = 1.6$ MHz, and $d_t = 5 \cdot 10^{13}$ cm^{-2}). The count rate for proton pairs is $R(\theta_1 < 2^\circ \,\mathrm{and}\, \theta_2 < 2^\circ) = L \cdot \sigma_{\mathrm{ce}} \cdot \varepsilon_{acc} \cdot \varepsilon_{\mathrm{det}}$, where $\sigma_{\mathrm{ce}} = 6.4$ mb is the mesonless CE cross section, $\varepsilon_{\mathrm{acc}} = 8.8 \cdot 10^{-3}$ is the FD acceptance resulting from simulations (Sec. 3.2.1), and $\varepsilon_{\mathrm{det}} \approx 50\%$ is the total detection efficiency based on previous experiments. These numbers yield $R(\theta_1 < 2^\circ \,\mathrm{and}\, \theta_2 < 2^\circ) = 2.2$ s^{-1}. For a sharper foward angle cut of 0.4°, corresponding to our angular resolution for protons, one gets approximately $R(\theta_1 < 0.4^\circ \,\mathrm{and}\, \theta_2 < 0.4^\circ) = 1/5^2 \cdot R(\theta_1 < 2^\circ \,\mathrm{and}\, \theta_2 < 2^\circ) = 0.09$ s^{-1}.

5.2 Request

Based on the HBC data from Ref. [43], at an incident deuteron beam energy of $T_d = 1.95$ GeV the number of events expected for different conditions are listed in Table 8.

- The **proposal requires a total of two weeks** to determine the differential cross

T_d [GeV]	$N_{pp}(0.4°)$/mode	$N_{pp}(2.0°)$/mode	N_{pp}(All)/mode	Time/mode [h]
1.95	3900	95000	392000	12

Table 8: Estimation of the expected number of events at ANKE for different conditions, based on Ref. [43], at an incident deuteron beam energy $T_d = 1.95$ GeV. $N_{pp}(0.4°)$ corresponds to the number of events in a forward cone $\theta_1 < 0.4°$ and $\theta_2 < 0.4°$. The term "mode" refers to the different polarisation modes of the polarised ion source.

section, and the tensor analysing powers T_{20} and T_{22} at four energies between $T_d = 1.2$ GeV and $T_d = 2.23$ GeV.

- With the **present request** the collaboration asks for **one week of beam time** to carry out measurements at two energies $T_d = 1.2$ and $T_d = 1.95$ GeV.

The measurements require to collect statistics in five different polarisation modes of the ion source (1, 2, 5, 10, and 11), thus we assume to take data for about 60 h at each energy. The inelastic cross section for dp interactions in this energy range does not vary more than $\approx 20\%$ [58].

6 Appendix

6.1 Polarised gas–target

Although the current proposal will be carried out with the hydrogen cluster target, the $\vec{d}\vec{p}$ spin–correlation studies envisaged in the continuation necessitate the availability of a polarised hydrogen target. A polarised storage cell gas target is being developed at IKP in collaboration with the St. Petersburg Nuclear Physics Institute, the Friedrich–Alexander–Universität Erlangen–Nürnberg, and the Universität zu Köln. A beam of polarised hydrogen (or deuterium) atoms from an atomic beam source (ABS) [66] will feed an open–ended storage cell. The polarisation axis of the atoms is given by the axis of quantisation in the vertical stray field of the spectrometer magnet D2. Transverse deuteron–beam and proton–target polarisation will allow us to study the reactions discussed in Sec. 2 and Sec. 4. A full amplitude determination requires longitudinally polarised protons in the target, which means developing an appropriate magnetic holding field at the polarised gas–target storage cell. The necessary homogeneous field has to extend over the full cell–tube length of about 40 cm. These difficult tasks require magnetic field calculations with use of, *e.g.* the MAFIA code during the design phase in order to optimise and complete a tentative first lay–out [67]. The field–shaping system has then to be built, installed and commissioned at ANKE.

References

[1] J. Bystricky et al., Nucl. Phys. A444 (1985) 597.

[2] R.A. Arndt et al., Phys. Rev. C62 (2000) 034005.

[3] M. Altmeier et al., Phys. Rev. Lett. 85 (2000) 1819.

[4] R.A. Arndt et al., Phys. Rev. C50 (1994) 2731; C56 (1997) 3005.

[5] A. de Lesquen et al., Eur. Phys. J C11 (1999) 69.

[6] V. Komarov et al., Phys. Lett. B553 (2003) 179.

[7] I. Pomeranchuk, Doklady Academii Nauk USSR, 78 (1951) 249.

[8] D.V. Bugg, C. Wilkin, Phys. Lett. B152 (1985) 37.

[9] D.V. Bugg, C. Wilkin, Nucl. Phys. A467 (1987) 575.

[10] G.C. Ohlsen, Rep. Prog. Phys. 35 (1972) 717.

[11] J. Carbonell, M.B. Barbaro and C. Wilkin, Nucl. Phys. A529 (1991) 653.

[12] M.B. Barbaro, C. Wilkin, J. Phys. G 15 (1989) L69.

[13] R. Dubois et al., Nucl. Phys. A377 (1982) 554.

[14] N.W. Dean, Phys. Rev. D5 (1972) 1661; Phys. Rev. D5 (1972) 2832.

[15] Yu.N. Uzikov. Annual Rep. IKP FZ Jülich, 2001 (2002) p.66.

[16] V. Franco, R. Glauber, Phys. Rev. 142 (1966) 1195.

[17] D. Bandyopadhyay et al., Phys. Rev. C40 (1989) 2684.

[18] J. Arnold et al., Eur. Phys. J. C17 (2000) 67.

[19] G. Glass et al., Phys. Rev. C47 (1993) 1369.

[20] J. Ball et al., Nuovo Cimento 111 (1998) 13.

[21] C. Lechanoine–Leluc and F. Lehar, Proceedings of conference: 'The 20 Years of the Synchrotron SATURNE–2', Paris 4–5 May, 1998. World Scientific (2000) p.96.

[22] P.R. Robrish et al., Phys. Lett. B31 (1970) 617.

[23] M.A. Abolins et al., Phys. Rev. Lett. 30 (1973) 1183.

[24] M.L. Marshak et al., Phys. Rev. C18 (1978) 331.

[25] Y. Makdisi et al., Phys. Rev. Lett. 45 (1980) 1529.

[26] R. Diebold et al., Phys. Rev. Lett. 35 (1975) 632.

[27] M. Sakuda et al., Phys. Rev. D25 (1982) 2004.

[28] J. Ball et al., Nucl. Instr. Meth. A381 (1996) 381.

[29] B.H. Silverman et al., Nucl. Phys. A499 (1989) 763.

[30] D.G. Grabb et al., Phys. Rev. Lett. 43 (1979) 983.

[31] I.P. Auer et al., Phys. Rev. Lett. 46 (1981) 1177.

[32] B.P. Adiasevich et al., Zeit. Phys. C 71 (1996) 65.

[33] H. Palevsky et al., Phys. Rev. Lett. 9 (1962) 509;
J.L. Friedes et al., Phys. Rev. Lett. 15 (1965) 38.

[34] R.E. Mischke et al., Phys. Rev. Lett. 23 (1969) 542.

[35] E.L. Miller et al., Phys. Rev. Lett. 26 (1971) 984.

[36] J. Engler et al., Phys. Lett. B34 (1971) 528.

[37] P.F. Shepard et al., Phys. Rev. D10 (1974) 2735.

[38] G. Bizard et al., Nucl. Phys. B85 (1975) 14.

[39] V. Böhmer et al., Nucl. Phys. B110 (1976) 205.

[40] A. Babaev et al., Nucl. Phys. B110 (1976) 189.

[41] R.D. Ransome et al., Phys. Rev. Lett. 48 (1982) 781.

[42] K.H. McNaughton et al., Phys. Rev. C48 (1992) 47.

[43] B. Aladashvili et al., Nucl. Phys. B86 (1975) 461.

[44] B. Aladashvili et al., J. Phys. G 3 (1977) 1225 .

[45] V.V. Glagolev et al., Eur. Phys. J. A15 (2002) 471.

[46] V.V. Glagolev et al., Part. Nucl. Lett. 100 (2000) 67.

[47] C. Wilkin and D.V. Bugg, Phys. Lett. B154 (1985) 243.

[48] S. Kox et al., Nucl. Phys. A556 (1993) 621.

[49] C. Ellegard et al., Phys. Rev. Lett. 59 (1987) 974.

[50] C. Ellegard et al., Phys. Lett. B231 (1989) 365.

[51] S.L. Belostotski et al., Phys. Rev. C56 (1997) 50.

[52] S. Barsov et al., Nucl. Instr. Meth. A462 (2001) 364.

[53] C. Kerboul, Phys. Lett. 181B (1986) 28.

[54] A. Khoukaz et al., Eur. Phys. J. D5 (1999) 275.

[55] U. Bechstedt et al., Operating report of COSY in 2000, IKP Annual Report, Jül–3852, 2000, p.143.

[56] S. Barsov et al., 'Study of ω-meson production', COSY proposal # 114, Spokesperson: R. Schleichert, (2002).

[57] S. Dymov et al., 'Near–threshold η production in $dd \to {}^4\mathrm{He}\,\eta$', COSY proposal # 107, Spokesperson: A. Wronska, (2002).

[58] N. Katayama et al. Nucl. Phys. A438 (1985) 685.

[59] A. Boudard, G. Fäldt, and C. Wilkin, Phys. Lett. B389 (1996) 440.

[60] M. Marshak et al., Phys. Rev. C18 (1978) 1.

[61] G. Korolev et al., Phys. Lett. 165B (1985) 4.

[62] V. Glagolev et al., VII Symposium on Spin Phenomena, Protvino, Sept.86, 1987, p.146 (JINR preprint P1-88-6)

[63] J. Arvieux et al., Nucl. Instr. Meth. A273 (1988) 48.

[64] V.N. Nikulin et al., Phys. Rev. C54 (1996) 1732.

[65] Collaboration ER54 *Nouvelles de Saturne* 13, 37 (1989).

[66] R. Emmerich et al., IKP Annual Report 2001 and earlier Annual reports; paper in preparation, to be submitted to Rev. Scient. Instr.

[67] V. Nelyubin, Proc. of Workshop on Proton–deuteron interaction studies, A. Kacharava, V. Komarov, F. Rathmann (eds.), Berichte des Forschungszentrum Jülich, 4012. ISSN 0944–2952, p. 189.